Published in final edited form as:
*Nature*. 2009 November 5; 462(7269): 104–107. doi:10.1038/nature08462.

# Requirement for NF-κB signaling in a mouse model of lung adenocarcinoma

**Etienne Meylan**, **Alison L. Dooley**, **David M. Feldser**, **Lynn Shen**, **Erin Turk**, **Chensi Ouyang**, and **Tyler Jacks**
Koch Institute for Integrative Cancer Research, and Department of Biology, and Howard Hughes Medical Institute, Massachusetts Institute of Technology, 77 Massachusetts Avenue, Cambridge, Massachusetts 02139, USA

## Summary

NF-κB transcription factors function as crucial regulators of inflammatory and immune responses as well as cell survival [1]. They have also been implicated in cellular transformation and tumorigenesis [2–6]. However, despite extensive biochemical characterization of NF-κB signaling during the past twenty years, the requirement for NF-κB in tumor development *in vivo*, particularly in solid tumors, is not completely understood. Here we show that the NF-κB pathway is required for the development of tumors in a mouse model of lung adenocarcinoma. Concomitant loss of p53 and expression of oncogenic K-ras$^{G12D}$ resulted in NF-κB activation in primary mouse embryonic fibroblasts. Conversely, in lung tumor cell lines expressing K-ras$^{G12D}$ and lacking p53, p53 restoration led to NF-κB inhibition. Additionally, inhibition of NF-κB signaling induced apoptosis in p53 null lung cancer cell lines. Inhibition of the pathway in lung tumors *in vivo*, from the time of tumor initiation or following tumor progression, resulted in significantly reduced tumor development. Together, these results suggest a critical function for NF-κB signaling in lung tumor development and, further, that this requirement depends on p53 status. These findings also provide support for the development of NF-κB inhibitory drugs as targeted therapies for the treatment of patients with defined mutations in K-ras and p53.

### Keywords

NF-κB; lung adenocarcinoma; mouse model

More than one million people die from lung cancer each year in the world, making it the leading cause of cancer mortality of both women and men. Non-small cell lung cancer (NSCLC) accounts for 80% of all lung cancer cases, with adenocarcinoma being the major subtype. NSCLC development is associated with frequent mutations in a few well-defined oncogenes and tumor suppressor genes. Oncogenic K-ras mutations occur in approximately 20–30% of

*Correspondence to:* Tyler Jacks, Koch Institute for Integrative Cancer Research, Massachusetts Institute of Technology, 77 Massachusetts Avenue, Cambridge, MA 02139, USA, Phone: +1 617 253 0263, Fax: +1 617 253 9863, tjacks@mit.edu.

**Supplementary Information** is linked to the online version of the paper at www.nature.com/nature.

**Author Contributions**
E.M. and T.J. designed the study, E.M., A.L.D., L.S. and E.T. performed the experiments, D.M.F. generated the mouse lung cancer model with restorable p53, C.O. generated lung cell lines from tumors of these mice, E.M. and T.J. analyzed the data, E.M. wrote the paper, A.L.D. and T.J. edited the paper.

**Author Information**
Reprints and permissions information is available at www.nature.com/reprints.

The authors declare no competing financial interests.

patients with lung adenocarcinoma, whereas inactivating mutations in the tumor suppressor protein p53 are found in at least 50% NSCLC cases [7]. The overexpression of oncogenic forms of Ras has been reported to result in NF-κB activation [3,8], while wild-type (WT) p53 has been shown to antagonize NF-κB activity [9–14]. Therefore, we hypothesized that induction of endogenous K-ras$^{G12D}$ or p53 deletion might affect the NF-κB signaling pathway. We used primary mouse embryonic fibroblasts (MEFs) carrying either the Cre-activatable K-ras$^{G12D}$ allele (*K-ras$^{Lox\text{-}STOP\text{-}Lox\ (LSL)\text{-}G12D/WT}$*), a conditional loss-of-function p53 allele (*p53$^{Flox/Flox}$*), or the two in combination (*K-ras$^{LSL\text{-}G12D/WT}$; p53$^{Flox/Flox}$*) [15–17]. Cells were infected with adenoviruses expressing either Cre (to activate oncogenic K-ras and/or inactivate p53) or FlpO recombinase (as a control). As shown in Figure 1a, activation of K-ras$^{G12D}$ with concomitant loss of p53 led to an increased nuclear accumulation of the NF-κB transcription factor subunit p65, a prerequisite for NF-κB activity. In contrast, p65 remained exclusively cytoplasmic upon K-ras$^{G12D}$ expression in WT p53-expressing cells or upon loss of p53 in the absence of K-ras$^{G12D}$ expression, suggesting that the combination of mutations is required for enhanced NF-κB activation, at least in these cells. Of note, another NF-κB subunit, c-Rel, showed a slight increase in nuclear localization upon p53 loss, both alone and upon K-ras$^{G12D}$ expression (Fig. 1a), perhaps reflecting crosstalk between p53 and c-Rel. We next addressed whether restoration of p53 expression in p53-mutant cells might influence p65 nuclear localization. We utilized K-ras$^{G12D}$-expressing lung adenocarcinoma cell lines with a Cre-activatable WT-p53 allele, which were derived from lung tumors of mice generated through the crossing of *K-ras$^{LA2/WT}$* (ref. [18]) and *p53$^{LSL/LSL}$; Cre-ER$^{T2}$* (ref. [19]) mice (D.M.F. and T.J., unpublished). In the absence of p53 restoration, nuclear p65 was evident in these cells, consistent with the data from MEFs (see Fig. 1a). Upon 4-hydroxytamoxifen-induced p53 restoration, p65 nuclear localization was diminished (Fig. 1b). In contrast, the nuclear levels of c-Rel remained unchanged. Reduced levels of nuclear p65 were not simply a consequence of cell cycle arrest, because p65 remained detectable in the nucleus of cells arrested through culturing in 0.1% serum. Importantly, restoration of p53 and decreased nuclear p65 were associated with reduced expression of the NF-κB-target gene *Tnf* (Fig. 1c). Expression of *Glut3*, which contributes to and is upregulated by NF-κB activity in p53-deficient MEFs [10], was also reduced upon restoration of p53 (Fig. 1c).

Using enzyme-linked immunosorbent assay (ELISA), we directly monitored NF-κB activity in lung adenocarcinoma cell lines derived from tumors generated in the conditional compound knock-in (*K-ras$^{LSL\text{-}G12D/WT}$; p53$^{Flox/Flox}$*) mouse. These mice (hereafter referred to as KP mice) develop advanced lung cancers that closely recapitulate the development of human lung adenocarcinoma [15]. In KP tumor cell lines, NF-κB p65 DNA-binding activity was consistently higher than in cell lines derived from the *K-ras$^{LA2/WT}$* allele (LKR), which also express K-ras$^{G12D}$ but retain WT p53 expression (Fig. 2a). We also examined NF-κB activity in human NSCLC cell lines that harbor gain-of-function mutations in K-ras but differ in their p53 status. Consistent with the mouse data, NF-κB p65 DNA-binding activity was increased in p53 mutant, compared to WT p53 cell lines, with one exception (Fig. 2b). Notably, nuclear p65 was higher in the p53 mutant cells (Supplementary Fig. 1). Hence, canonical NF-κB signaling is elevated in lung tumor-derived cells with altered p53.

To determine if NF-κB provides pro-survival signals in KP cell lines, we examined the consequences of pathway inhibition. Cell viability was monitored following infection of cells with lentiviruses expressing a non-phosphorylatable, dominant-negative form of IκBα (Super Repressor, IκB-SR). As shown in Figure 3a, expression of IκB-SR led to reduced KP cell viability. In contrast, the two LKR cell lines expressing mutant K-ras and WT p53 (LKR10 and LKR13) were insensitive to IκB-SR expression. These results are consistent with the data showing increased NF-κB activity in KP cells (see Fig. 2a). NF-κB signaling was also inhibited via shRNA-mediated knock-down of NEMO, an essential factor in the canonical NF-κB pathway [20,21]. Infection of LKR, KP and 3TZ fibroblast cell lines with pSicoRev retroviral

vectors [22] expressing one of two hairpins targeting NEMO resulted in efficient knock-down in all cases, while apoptosis (as measured by cleaved caspase-3 detection) was only triggered in the KP cell line (Fig. 3b). To establish if one of the two NF-κB subunits, p65 or c-Rel, transmitted these anti-apoptotic effects, we used shRNA-mediated knock-down to inhibit them in the same cells. Knock-down of p65, but not of c-Rel, led to reduced cell viability and cleavage of caspase-3 (Fig. 3c,d). These results demonstrate that in the context of oncogenic K-ras expression and p53 mutation, the canonical NEMO-, IκB- and p65-dependent NF-κB signaling pathway is required for survival of lung cell lines.

In order to understand the relevance of these findings *in vivo*, we examined the NF-κB signaling pathway during lung adenocarcinoma development in KP mice. Tumors from KP mice exhibited enhanced NF-κB p65 nuclear localization by immunohistochemistry when compared to tumors from K-ras$^{G12D}$ mice (*K-ras$^{LSL\text{-}G12D/WT}$*, Supplementary Fig. 2). To test the functional requirement for NF-κB in tumor initiation and development, we infected KP mice with a bi-functional lentivirus capable of expressing both IκB-SR and Cre constitutively from independent promoters or a control lentivirus carrying only Cre (Supplementary Fig. 3a). Each mouse was either infected with low- ($5\times10^3$) or high-titer ($5\times10^4$) lentiviral particles. Seventeen weeks after infection with low titer control viruses, an average of 30 tumors were detected per mouse (Fig. 4a, left), whereas mice infected with lentiviruses expressing Cre and IκB-SR had either a single tumor or none at all. Using the high titer lentiviruses, a similarly dramatic difference between Cre- and IκB-SR-Cre-infected mice was observed (90–131 tumors compared to 6–22; Fig. 4a, right). Thus, inhibition of NF-κB at the time of tumor initiation in the KP mouse model had a profound effect on subsequent tumor development. To determine if NF-κB was required to maintain the growth and/or viability of established tumors, we cloned IκB-SR into a lentiviral construct downstream of a tetracycline-response element (TRE), to generate a doxycycline (dox)-inducible version of IκB-SR (see Supplementary Fig. 3a,b). KP mice were crossed to clara cell secretory protein (CCSP)-rtTA transgenic mice, which express the reverse tetracycline transactivator (rtTA) specifically in lung epithelial cells [23]. *KP; CCSP-rtTA+* mice and *KP; CCSP-rtTA−* littermate controls were infected with TRE.IκB-SR; Pgk.Cre lentiviruses to initiate tumorigenesis. In an initial experiment, infected mice were put on a dox diet continuously from the day of infection. Fifteen weeks later, lung tumor development was analyzed using *in vivo* micro-computed tomography (μ-CT) imaging. As we observed with constitutive IκB-SR expression, dox-mediated IκB-SR induction from the time of tumor initiation led to significant impairment of tumor development (Fig. 4b). To address the role of NF-κB in tumor maintenance, cohorts of infected mice were imaged by μ-CT at 15 weeks post-infection to establish pre-treatment lung tumor volumes. One week later, the mice were placed on a dox diet to induce the expression of IκB-SR specifically in the tumor cells and imaged weekly for a total of five weeks. As shown in Figure 4c, IκB-SR expression resulted in a significantly diminished tumor growth rate over time compared to controls. Thus, established tumors with an activating mutation in K-ras and loss of p53 function are sensitive to NF-κB inhibition.

To begin to explore the effects of NF-κB inhibition in this system, we examined the expression levels of certain NF-κB target genes by real-time PCR after one week of dox treatment, starting at 14 weeks post-infection. Of note, *IκBα* levels (which correspond to both endogenous *IκBα* and the exogenous *IκB-SR*) were about 5-fold higher in IκB-SR-expressing tumors, demonstrating the efficiency of the dox-inducible system (Fig. 4d and Supplementary Table 1). Contrary to our expectations, the expression of three NF-κB targets that inhibit apoptosis, *Bcl2*, *Bclx* and *Xiap*, did not significantly change following dox treatment. In contrast, *Tnf* and *Il6* mRNA levels were increased in tumors expressing IκB-SR. The induction of these inflammatory genes is likely due to infiltrating inflammatory cells recruited to tumors in which NF-κB has been inhibited (Supplementary Fig. 4). Such inflammatory response has been

observed upon NF-κB repression in liver and intestinal epithelial cells [4,24]. Future experiments will examine the importance of inflammation in the anti-tumor response.

Lung cancer is the leading cause of cancer death in the world. To develop more effective treatments, it is essential to characterize the pathways that control tumor cell proliferation and survival, which will differ depending on the specific genetic context of individual tumors. Our data establish a critical role for the NF-κB pathway in lung cancer cells harboring mutations in the commonly mutated genes, K-ras and p53. These results, which corroborate earlier studies demonstrating the importance of NF-κB signaling in a chemical-induced lung tumor model [25], provide a basis to consider the pharmacological inhibition of the NF-κB pathway in the treatment of lung cancer. Because canonical NF-κB signaling serves anti-inflammatory and immunosuppressive functions in macrophages [26,27], phenotypes that are regularly observed in tumor-associated macrophages, NF-κB inhibition might serve dual functions. Indeed, NF-κB inhibition may directly affect tumor epithelial cell survival and the tumor microenvironment, by recruiting and/or converting neutrophils or macrophages toward pro-inflammatory and tumoricidal phenotypes.

The therapeutic inhibition of NF-κB has been viewed with caution upon the discovery of diverse functions of this pathway in different physiological instances [28]. Our study suggests a re-evaluation of the importance of targeting NF-κB in cancer. With an *a priori* knowledge of the genetic mutations of the tumors, treatment with NF-κB inhibitors may become an important option of targeted therapy for lung cancer.

## Methods summary

### Mice

*K-ras*$^{LSL\text{-}G12D/WT}$*; p53*$^{Flox/Flox}$ (KP), *p53*$^{LSL/LSL}$*; Cre-ER*$^{T2}$ and *K-ras*$^{LA2}$ mice have been described earlier [15,18,19]. To generate a lung adenocarcinoma mouse model with restorable p53, *p53*$^{LSL/LSL}$*; Cre-ER*$^{T2}$ mice were crossed to *K-ras*$^{LA2}$ mice (D.M.F. and T.J., not published). *CCSP-rtTA* mice [23], purchased from the Jackson Laboratory, were crossed to KP mice. 625 doxycycline diet was from Harlan Laboratories. Mouse research was approved by the Committee for Animal Care, and conducted in compliance with the Animal Welfare Act Regulations and other Federal statutes relating to animals and experiments involving animals and adheres to the principles set forth in the *Guide for the Care and Use of Laboratory Animals*, National Research Council, 1996 (institutional animal welfare assurance no. A-3125–01).

### Virus production and infection

293T cells were transfected using Fugene (Roche) with pMD2G (VSV-G protein), Δ8.2 (lentivirus packaging vector, kindly provided by I. Verma, Salk Institute, La Jolla, California) and expression plasmid. Viral supernatants were harvested 48 and 72 hours post-transfection, filtered, and used directly for infection of cell lines. For mouse experiments, virus preparation and mouse infection protocols were previously described [29]. 2- to 3-month old mice were intratracheally infected with $5\times10^3$, $10^4$ or $5\times10^4$ lentiviral particles, or with $10^7$ adenoviral particles expressing Cre (AdCre), as indicated.

## Methods

### Measurement of lung tumor volumes

Mice were anesthetized using isoflurane, and were under anesthesia during the entire scanning procedure. Lungs were imaged at the Koch Institute Microscopy and Imaging Core Facility by μ-CT. Image acquisition was performed using eXplore Scan Control software, using a 45 μm

voxel size program, and 3D reconstruction was performed using eXplore Reconstruction Utility software (both from GE Healthcare). High-resolution files of the lung scans were generated and individual tumor volumes were measured and calculated using MicroView software (GE Healthcare). For Fig. 4b, the lung surface opacity was set to 25%.

### Histology and immunohistochemistry

Mouse lungs were inflated and then fixed in 3.6% formaldehyde in PBS for 24 hours, transferred to 70% EtOH, and embedded in paraffin. 4 μm tissue sections were either deparaffinized and stained with hematoxylin and eosin to count tumor numbers (Fig. 4a), or used for immunohistochemistry. In this case, sections were deparaffinized, boiled in 10 mM Na-citrate, washed in $H_2O$, treated with 1% $H_2O_2$ for 10 minutes, washed in $H_2O$ and in PBS. Blocking was done for 1 hour in PBS with 5% goat serum, followed by incubation with anti-p65 antibodies (C-20, 1/200) for 1 hour, then by washing and staining with biotin-conjugated secondary antibodies (1 hour). After washing, avidin-biotinylated HRP complexes were added during 30 minutes (ABC kit, Vectastain), and the complexes were revealed with a DAB peroxidase substrate kit (#SK-4100, Vector Laboratories). The tissues were counterstained with methyl green and mounted.

### Expression vectors

Super Repressor IκB (IκB-SR) was cloned from a mouse expressed sequenced tag with a 5' oligo that added an EcoRI site followed by a Kozak sequence prior to the START codon, and mutating codons for Ser32 and Ser36 into Alanine-encoding ones. The 3' oligo introduced a silent mutation removing an EcoRI site in the gene sequence, deleted the IκB STOP codon, added a FLAG tag sequence followed by a STOP and a NotI site. IκB-SR was amplified using Pfx polymerase (Invitrogen), and was cloned into EcoRI-NotI sites located next to a UbC promoter in a dual-promoter lentiviral vector that also expresses Cre from the Pgk promoter. To generate a doxycycline-responsive FLAG-IκB-SR version, IκB-SR was PCR amplified with oligos adding EcoRI sites on both ends, and cloned into an EcoRI-digested TRE; Pgk.Cre lentiviral vector (pCW22), downstream of the TRE promoter. shRNAs to NEMO, c-Rel and p65 were designed by the pSICOLIGOMAKER 1.5 program (http://web.mit.edu/jacks-lab/protocols/pSico.html; created by A. Ventura, Memorial Sloan-Kettering Cancer Center, New York). Oligos were annealed and ligated into pSicoRev retroviral vectors, as described [22]. The fidelity of the PCR amplifications and oligo syntheses were confirmed by sequencing.

### Cell culture conditions

The human embryonic kidney (HEK) 293T and mouse fibroblasts 3TZ cells were grown in Dulbecco's modified Eagle's Medium (DMEM). LKR (LKR10, LKR13) and KP cell lines were grown in Minimum Essential Medium (MEM). Lung cells derived from *K-ras*$^{LA2/WT}$*; p53*$^{LSL/LSL}$*; Cre-ER*$^{T2}$ (not published) tumors were grown in DMEM. A549 and SW1573 cell lines were grown in a 1:1 mixture of F12 and DMEM. H23, H2122, H441, H460, Calu-6, H1944, H2009 and H727 were grown in RPMI. All human cell lines were obtained from the ATCC. Early passage mouse embryonic fibroblasts (MEFs, all obtained from the indicated genotypes in pure 129 backgrounds) were cultured with DMEM. All cell media were supplemented with 1% glutamine, 50 units/ml penicillin, 50 μg/ml streptomycin and 10% heat inactivated FBS.

### Statistics

P-values were all determined by Student's t tests.

### Nuclear-cytoplasmic fractionations

Cells in 10 cm dishes were washed with cold PBS and harvested by scraping following addition of lysis buffer A (HEPES pH 7.6 20 mM, 20% glycerol, 10 mM NaCl, 1.5 mM $MgCl_2$, 0.2 mM EDTA, 1 mM DTT, 0.1% NP-40, and a proteinase inhibitor cocktail (Roche)). Lysis was completed on ice for 10 minutes. Supernatants containing the cytoplasmic fractions were collected after centrifugation (2000 rpm, 4°C, 5 minutes). The pellets were washed three times in lysis buffer A and then lysed in buffer B (HEPES pH 7.6 20 mM, 20% glycerol, 500 mM NaCl, 1.5 mM $MgCl_2$, 0.2 mM EDTA, 1 mM DTT, 0.1% NP40, and a proteinase inhibitor cocktail (Roche)) for 30 minutes on ice. After centrifugation (13000 rpm, 4°C, 15 minutes), the recovered supernatants containing the nuclear lysates were collected and frozen (−70°C) until use. For Fig. 1a, the data are representative of two independent experiments each performed on two different MEF preparations. For Fig. 1b, the data are representative of results obtained from three independent cell lines.

### Cell viability assay

Cells were split into 96-well plates (3000 cells per well). 24 hours later, cells were infected with the indicated retro- or lentiviruses, and 72 hours later cells were fixed in Methanol (10 minutes), dried 15 minutes, stained 10 minutes in Methylene blue dye (0.05% Methylene blue in 1× borate buffer (borate buffer 10×, pH8.4, consists of 100 mM $H_3BO_3$, 25 mM $Na_2BO_7$, 120 mM NaCl)), washed three times under gentle tap water, and dried (2 hours, 37°C). 0.1 M HCl was added for solubilization, after which cell viability was measured on a spectrophotometer (O.D. 650 nm). Non-infected cell values were set to 1 (100% viability).

### RNA purification, reverse transcription and real-time PCR amplification

RNA was purified using Trizol (Invitrogen), according to the manufacturer's instructions. 1 μg RNA was reverse-transcribed using a High-Capacity cDNA Reverse Transcription Kit (Applied Biosystems). 10 ng cDNA was used for real-time PCR amplification, using commercially available Taqman probes for mouse *Gapdh*, *Tnf*, *Glut3*, *Ikba*, *Bcl2*, *Bclx*, *Xiap*, *Il6* and *Cxcl1* (Applied Biosystems). Data were normalized to the *Gapdh* levels, and analyzed using the comparative $C_T$ method [30], except for Fig. 4d, where data are presented as fold changes ($2^{-\Delta CT}$ (rtTA+)/$2^{-\Delta CT}$ (rtTA−); mean rtTA− set to 1).

### NF-κB p65 DNA-binding activity assay

5 μg of nuclear extracts were used to determine p65 DNA-binding activity using an ELISA-based assay, according to the manufacturer's instructions (Active Motif TransAM, #40096). Briefly, κB oligonucleotide-coated plates (in a 96-well format) were incubated for 1 hour with the nuclear extracts. Specificity was achieved through incubation with anti-p65 primary antibodies for 1 hour. HRP-conjugated secondary antibodies were used for the detection of p65 bound to the κB sequences.

### Reagents

Mouse TNF (used at 50 ng/ml) was from Apotech. Antibodies to cleaved caspase-3 (#9661), IKKβ (2C8) and PARP (46D11) were purchased from Cell Signaling. Antibodies to p65 (C-20), c-Rel (C) and NEMO (FL-419) were purchased from Santa Cruz. Mouse anti-p53 was a kind gift from K. Helin (Copenhagen, Denmark). Rabbit anti-Flag (F7425) antibodies, 4-hydroxytamoxifen and doxycycline were purchased from Sigma.

### Infection of MEFs

In Fig. 1a, primary MEFs (passage 2) of the indicated genotypes were infected with adenoviruses (100 MOI) expressing Cre recombinase (AdCre) or FlpO recombinase (AdFlpO)

(University of Iowa, Gene Transfer Vector Core, http://www.uiowa.edu/~gene/). 6 days later, cells were harvested and subjected to the cytoplasmic-nuclear fractionation protocol.

## Supplementary Material

Refer to Web version on PubMed Central for supplementary material.

## Acknowledgments

We thank D. McFadden, T. Oliver, M. DuPage, K. Lane, A. Cheung, M. Kumar and E. Snyder for stimulating discussions and for generously sharing various reagents, A. Deconinck for critical reading of the manuscript, D. Crowley (Koch Institute Histology Core Facility) for preparation of tissue sections, and the entire Jacks laboratory for helpful discussions. This work was supported by the Howard Hughes Medical Institute (T.J.) and partially by a Cancer Center Support grant from the NCI (P30-CA14051). T.J. is the David H. Koch Professor of Biology and a Daniel K. Ludwig Scholar. E.M. is a recipient of fellowships from the International Human Frontier Science Program Organization and the Swiss National Science Foundation. D.M.F. is a recipient of a Leukemia & Lymphoma Society Fellow Award.

## References

1. Hayden MS, Ghosh S. Signaling to NF-kappaB. Genes Dev 2004;18:2195–2224. [PubMed: 15371334]
2. Greten FR, et al. IKKbeta links inflammation and tumorigenesis in a mouse model of colitis-associated cancer. Cell 2004;118:285–296. [PubMed: 15294155]
3. Hanson JL, Hawke NA, Kashatus D, Baldwin AS. The nuclear factor kappaB subunits RelA/p65 and c-Rel potentiate but are not required for Ras-induced cellular transformation. Cancer Res 2004;64:7248–7255. [PubMed: 15492243]
4. Luedde T, et al. Deletion of NEMO/IKKgamma in liver parenchymal cells causes steatohepatitis and hepatocellular carcinoma. Cancer Cell 2007;11:119–132. [PubMed: 17292824]
5. Maeda S, Kamata H, Luo JL, Leffert H, Karin M. IKKbeta couples hepatocyte death to cytokine-driven compensatory proliferation that promotes chemical hepatocarcinogenesis. Cell 2005;121:977–990. [PubMed: 15989949]
6. Pikarsky E, et al. NF-kappaB functions as a tumour promoter in inflammation-associated cancer. Nature 2004;431:461–466. [PubMed: 15329734]
7. Herbst RS, Heymach JV, Lippman SM. Lung cancer. N Engl J Med 2008;359:1367–1380. [PubMed: 18815398]
8. Finco TS, et al. Oncogenic Ha-Ras-induced signaling activates NF-kappaB transcriptional activity, which is required for cellular transformation. J Biol Chem 1997;272:24113–24116. [PubMed: 9305854]
9. Huang WC, Ju TK, Hung MC, Chen CC. Phosphorylation of CBP by IKKalpha promotes cell growth by switching the binding preference of CBP from p53 to NF-kappaB. Mol Cell 2007;26:75–87. [PubMed: 17434128]
10. Kawauchi K, Araki K, Tobiume K, Tanaka N. p53 regulates glucose metabolism through an IKK-NF-kappaB pathway and inhibits cell transformation. Nat Cell Biol 2008;10:611–318. [PubMed: 18391940]
11. Kawauchi K, Araki K, Tobiume K, Tanaka N. Loss of p53 enhances catalytic activity of IKK{beta} through O-linked {beta}-N-acetyl glucosamine modification. Proc Natl Acad Sci U S A. 2009
12. Ravi R, et al. p53-mediated repression of nuclear factor-kappaB RelA via the transcriptional integrator p300. Cancer Res 1998;58:4531–4536. [PubMed: 9788595]
13. Wadgaonkar R, et al. CREB-binding protein is a nuclear integrator of nuclear factor-kappaB and p53 signaling. J Biol Chem 1999;274:1879–1882. [PubMed: 9890939]
14. Webster GA, Perkins ND. Transcriptional cross talk between NF-kappaB and p53. Mol Cell Biol 1999;19:3485–3495. [PubMed: 10207072]
15. Jackson EL, et al. The differential effects of mutant p53 alleles on advanced murine lung cancer. Cancer Res 2005;65:10280–10288. [PubMed: 16288016]

16. Jackson EL, et al. Analysis of lung tumor initiation and progression using conditional expression of oncogenic K-ras. Genes Dev 2001;15:3243–3248. [PubMed: 11751630]
17. Jonkers J, et al. Synergistic tumor suppressor activity of BRCA2 and p53 in a conditional mouse model for breast cancer. Nat Genet 2001;29:418–425. [PubMed: 11694875]
18. Johnson L, et al. Somatic activation of the K-ras oncogene causes early onset lung cancer in mice. Nature 2001;410:1111–1116. [PubMed: 11323676]
19. Ventura A, et al. Restoration of p53 function leads to tumour regression in vivo. Nature 2007;445:661–665. [PubMed: 17251932]
20. Rothwarf DM, Zandi E, Natoli G, Karin M. IKK-gamma is an essential regulatory subunit of the IkappaB kinase complex. Nature 1998;395:297–300. [PubMed: 9751060]
21. Yamaoka S, et al. Complementation cloning of NEMO, a component of the IkappaB kinase complex essential for NF-kappaB activation. Cell 1998;93:1231–1240. [PubMed: 9657155]
22. Ventura A, et al. Cre-lox-regulated conditional RNA interference from transgenes. Proc Natl Acad Sci U S A 2004;101:10380–10385. [PubMed: 15240889]
23. Perl AK, Tichelaar JW, Whitsett JA. Conditional gene expression in the respiratory epithelium of the mouse. Transgenic Res 2002;11:21–29. [PubMed: 11874100]
24. Nenci A, et al. Epithelial NEMO links innate immunity to chronic intestinal inflammation. Nature 2007;446:557–561. [PubMed: 17361131]
25. Stathopoulos GT, et al. Epithelial NF-kappaB activation promotes urethane-induced lung carcinogenesis. Proc Natl Acad Sci U S A 2007;104:18514–18519. [PubMed: 18000061]
26. Fong CH, et al. An antiinflammatory role for IKKbeta through the inhibition of "classical" macrophage activation. J Exp Med 2008;205:1269–1276. [PubMed: 18490491]
27. Hagemann T, et al. "Re-educating" tumor-associated macrophages by targeting NF-kappaB. J Exp Med 2008;205:1261–1268. [PubMed: 18490490]
28. Pikarsky E, Ben-Neriah Y. NF-kappaB inhibition: a double-edged sword in cancer? Eur J Cancer 2006;42:779–784. [PubMed: 16530406]
29. Dupage M, Dooley AL, Jacks T. Conditional mouse lung cancer models using adenoviral or lentiviral delivery of Cre recombinase. Nat Protoc 2009;4:1064–1072. [PubMed: 19561589]
30. Schmittgen TD, Livak KJ. Analyzing real-time PCR data by the comparative C(T) method. Nat Protoc 2008;3:1101–1108. [PubMed: 18546601]

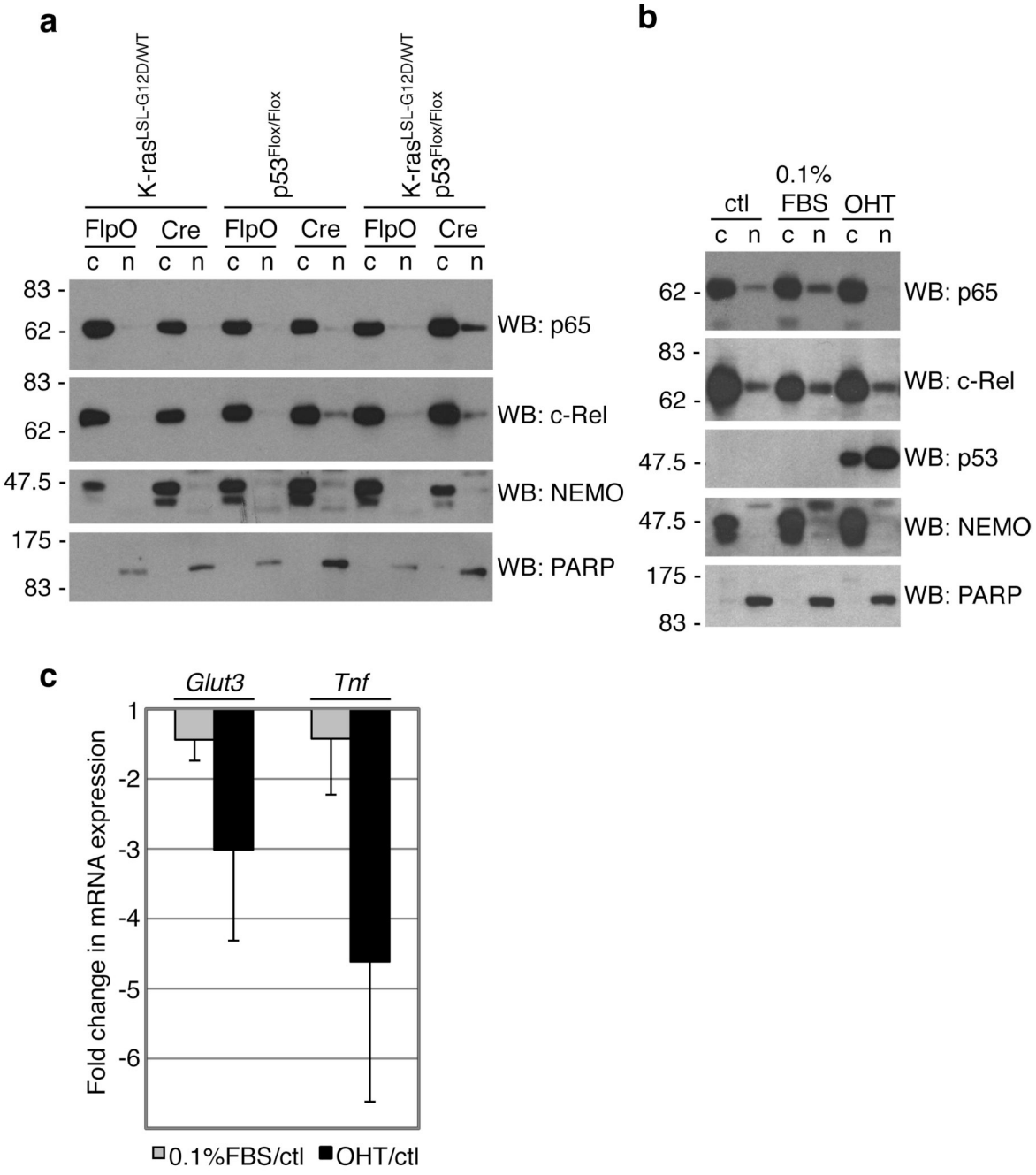


**Figure 1.**

NF-κB activity depends on p53. (**a**) MEFs were infected with adenoviruses expressing Cre or FlpO recombinase. 6 days later, cytoplasmic (c) and nuclear (n) lysates were analyzed by western blot (WB). NEMO (cytoplasmic) and PARP (nuclear) were used to determine purity. (**b,c**) *K-ras*$^{LA2/WT}$*; p53*$^{LSL/LSL}$*; Cre-ER*$^{T2}$–lung tumor derived cells were either untreated (ctl), cultured in 0.1% FBS or stimulated with 200 nM 4-hydroxytamoxifen (OHT). (**b**) 4 days later, cells were lysed and analyzed as in (**a**). (**c**) 4 days later, RNA was purified, reverse transcribed, and cDNA was amplified using probes for *Glut3, Tnf* or *Gapdh* (internal control). Data show means +/− s.d. (n= 3 independent cell lines), presented as fold changes (treatment/control; see Methods) [30].

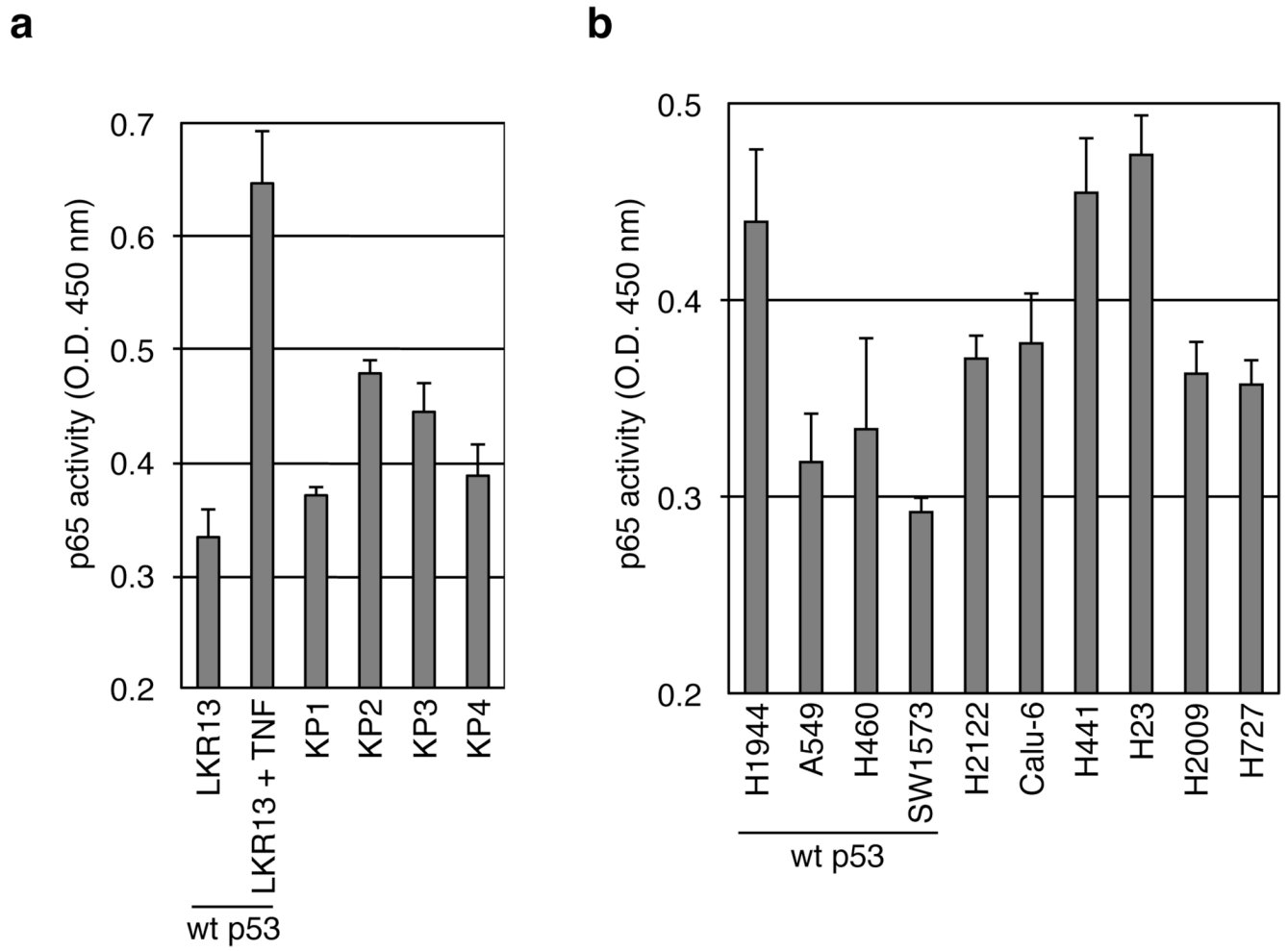


**Figure 2.**

NF-κB p65 DNA-binding activity is increased in NSCLC cells with altered p53. (**a,b**) 5 μg of nuclear lysates of the indicated mouse (**a**) or human (**b**) cell lines were analyzed for p65 DNA-binding activity by an ELISA assay (see Methods). Cells harboring WT p53 are indicated. As a positive control of p65 activity, LKR13 cells (**a**) were stimulated with TNF for 30 minutes prior to lysis.

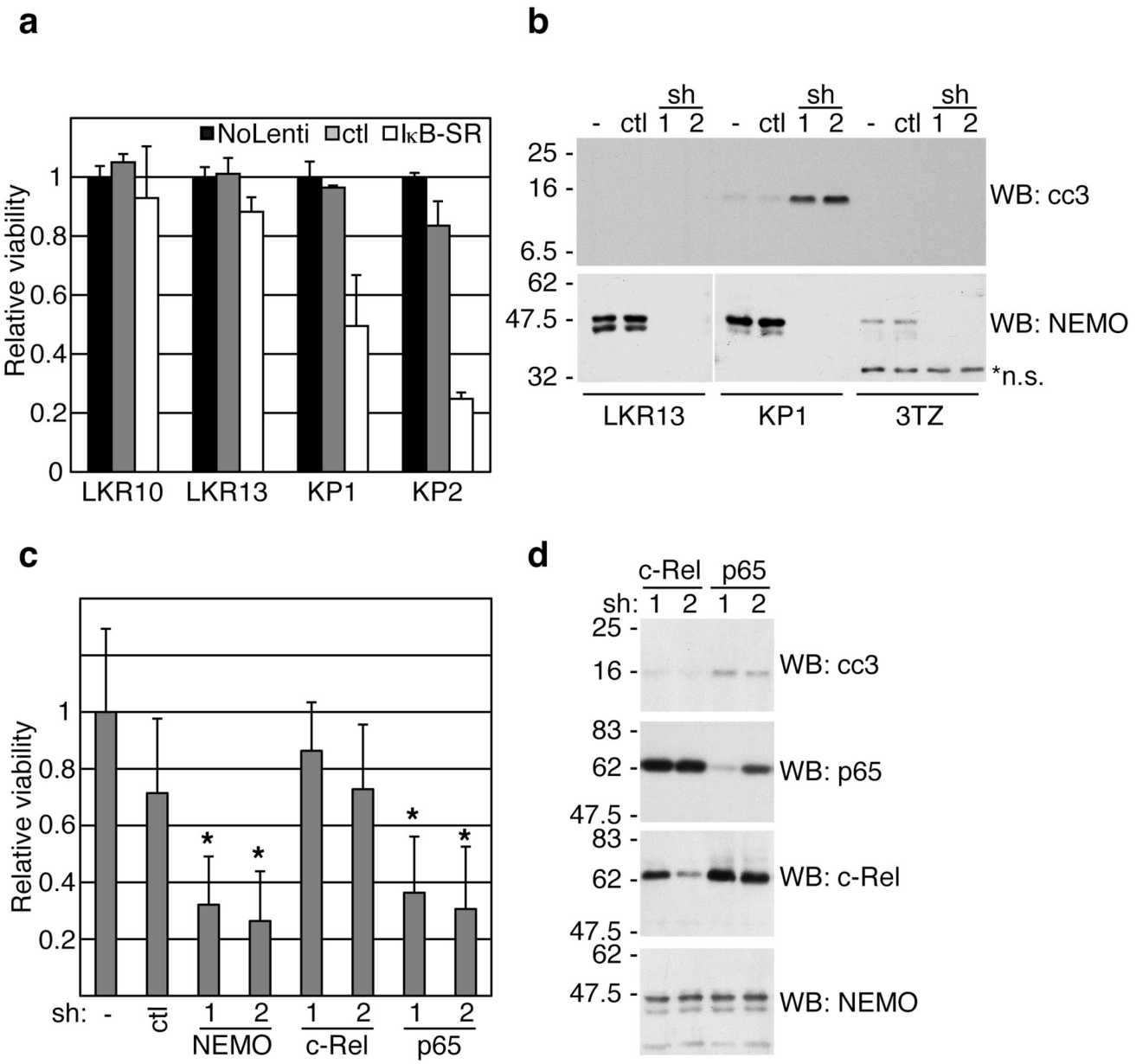


**Figure 3.**

NF-κB inhibition results in apoptosis of p53-deficient lung adenocarcinoma cells. (**a**) Two WT p53 (LKR10 and LKR13) and two *K-ras*$^{LSL\text{-}G12D/WT}$*; p53*$^{Flox/Flox}$ (KP) mouse cell lines were uninfected (No Lenti), infected with control (ctl) or IκB-SR expressing lentiviruses. 72 hours later, cells were assayed for viability (see Methods). Data are means +/− s.d. (n=3) of cell viability relative to uninfected cells (set to 1). (**b**) Lung cell lines or fibroblasts (3TZ) were untreated (−) or infected with pSicoRev expressing a *Nemo* (sh1, 2) or ctl hairpin. 72 hours later, cell extracts were analyzed by WB. *n.s., non-specific staining. (**c,d**) KP cells were infected with pSicoRev expressing the indicated hairpin, or were uninfected (−). 72 hours later, cells were assayed for viability (*c*), or cell extracts were analyzed by WB (**d**). (*c*) Data are means +/− s.d. (n=6) of cell viability relative to uninfected cells (set to 1). *, P<0.05 relative to ctl hairpin.

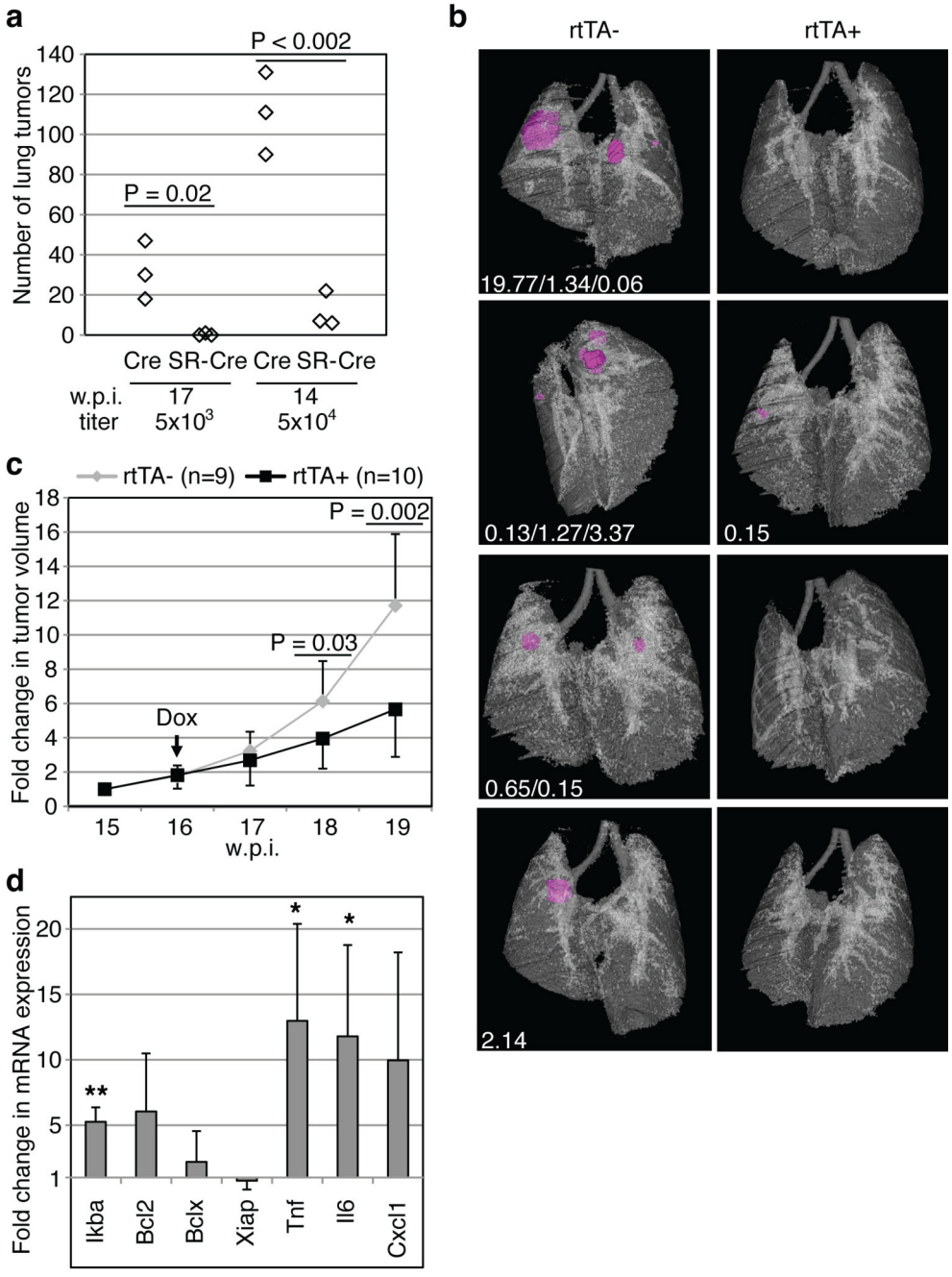


**Figure 4.**

NF-κB inhibition impairs lung adenocarcinoma development. (**a**) *K-ras*$^{LSL\text{-}G12D/WT}$*; p53*$^{Flox/Flox}$ mice were infected with Lenti-Pgk.Cre or Lenti-UbC.IκB-SR; Pgk.Cre viruses, sacrificed 17 (left) or 14 (right) weeks post-infection (w.p.i.) and tumor number was counted (see Methods). (**b**–**d**) *K-ras*$^{LSL\text{-}G12D/WT}$*; p53*$^{Flox/Flox}$*; CCSP-rtTA*+ (rtTA+) or *-rtTA*− mice (rtTA−) were infected with Lenti-TRE.IκB-SR; Pgk.Cre viruses ($10^4$ viral particles). (**b**) From the day of infection, mice were fed a doxycycline diet (Dox). At 15 w.p.i., μ-CT imaged tumors (magenta) and lungs were reconstructed and individual tumor volumes ($mm^3$, white text) were measured. (**c**) From 15 to 19 w.p.i., lungs were μ-CT imaged, and individual tumor volumes were measured. Data points represent means of fold change +/− s.d. in tumor volume relative

to 15 w.p.i. (set to 1). (**d**) After one week of Dox treatment, RNA was isolated from tumors of rtTA+ (n=4) or rtTA− (n=3) mice. cDNA was amplified using probes for the indicated genes or *Gapdh* (internal control). Data show means +/− s.d. **, P=0.001; *, P=0.04 (*Tnf*) or 0.05 (*Il6*).